Light Scattering by Bovine α-Crystallin Proteins in Solution: Hydrodynamic Structure and Interparticle Interaction

Jia-zhi Xia, Tony Aerts, Kristin Donceel, and Julius Clauwaert
Biophysics Research Group, Department of Biochemistry, University of Antwerp, U.I.A., B-2610 Antwerp, Belgium

ABSTRACT We have studied diluted bovine eye lens α-crystallin solutions by using light scattering. The protein particles were modeled as hard spheres, showing electrostatic repulsion, due to surplus electric charges, and weak attractive interaction. The repulsive potential V_R is defined by the radius of the particles, the Debye length κ^{-1}, and the number of charges at the Gouy layer; the attractive potential has been described by the London–van der Waals potential and is defined by the Hamaker constant A. We have used the diluted gas approximation and the one component macrofluid model to relate the experimental static factor K_I to the theoretical expression of the interaction potential $V(x)$. This resulted in a Hamaker constant A of 0.06 ± 0.01 K_BT and an effective charge q ranging from 18 ± 1 at low ionic strength (Ω = 0.0022 M) to 50 ± 5 at high ionic strength (Ω = 0.1472 M).

INTRODUCTION

The major role of the cytoplasm of the vertebrate eye lens fiber cell is to form a high refractive transparent medium so that the lens can contribute to focus the images on the retina. This high refractive medium (n ranging from 1.37 to 1.44) is obtained by a high concentration of soluble proteins. An approximation of this protein concentration can be obtained from the relation

$$n = n_0 + \frac{\partial n}{\partial c} \cdot \Delta c. \quad (1)$$

If we take n_0 = 1.33 and $\partial n/\partial c$ = 0.200 ml/g, we obtain a protein concentration Δc ranging from 20 to 55 g/100 ml. The lens crystallins are the main contributors to this high protein concentration; they form a complex system that can be divided into three main subclasses based on size and isoelectric point: α-, β-, and γ-crystallins (Bloemendal, 1981).

In spite of this high protein content, the eye lens is virtually completely transparent under normal, healthy conditions. A theoretical explanation for this apparent contradiction was given by Benedek in the early 1970s (Benedek, 1971). He showed that a limited degree of order in the lens cytoplasm could account for the observed transparency. This was proven experimentally to be correct by Delaye and Tardieu more than a decade later (Delaye and Tardieu, 1983). To explain this short range order of this highly concentrated protein solution on a quantitative basis, the hydrodynamic structure and the interparticle interaction of the proteins has to be known.

The α-crystallins are present in the highest concentration in the cytoplasm and they have also the highest molecular mass, so they play a key role in the eye lens light scattering and transparency. The study of homogeneous α-crystallin solutions, in well-defined solvent conditions, allows quantitative conclusions about the solution behavior of this protein. Static light scattering on diluted solutions is used to determine the molecular mass and hydrodynamic radius of the α-crystallin proteins in solvents with different ionic strengths. In these conditions and by extrapolation to a concentration of 0, the undisturbed molecular properties can be obtained. These molecular properties are the cornerstones for the interpretation of studies of solutions at low, medium, and high concentrations. In these conditions, the solution properties are influenced by the interparticle interactions so the light scattering and hydrodynamic properties are now in a more complex way related to the properties of the single molecules and their concentration. Here the interparticle interactions have to be taken into account.

The surface potential of the particles is a key factor in the interaction between two protein particles: if accepting a spherical particle, the surface potential is defined by the radius of the spherical particle, which can be calculated from the diffusion coefficient and the molecular mass, and further by the charge density. Many authors have proposed theoretical expressions to calculate the surface potential and interaction potential as a function of the properties of the charged particles (radius of the sphere and charge density) and the concentration of surrounding counterions (Verwey and Overbeek, 1948; Corti and Degiorgio, 1981; Oshima et al., 1982).

We have used static light scattering of diluted solutions to study the interaction between the protein particles at low, medium, and high ionic strength solvents. We have used the Derjaguin-Landau-Verwey-Overbeek potential and the one component macrofluid liquid model for the theoretical analysis of the protein solutions (Dorshow and Nicoli, 1981). By fitting the experimental data to theoretical expressions, which take into account the electrostatic interaction, it was

Received for publication 14 June 1993 and in final form 8 December 1993.
This work was supported by grants from the Fund for Joint Basic Research (FKFO) and the Fund for Medical Scientific Research (FGWO). This work was performed within the framework of Eurage (EEC concerted action on cellular aging and diseases).

Address reprint requests to Dr. J. Clauwaert, Biophysics Research Group, Department of Biochemistry, University of Antwerp, Universiteitsplein 1, B-2610 Antwerp, Belgium.

0006-3495/94/03/861/12 $2.00

possible to get a quantitative estimate of the electrostatic repulsion between the charged particles; however, our experiments at high ionic strength revealed the presence of an attractive interaction. Therefore the interaction between the α-crystallins is a delicate balance between hard sphere interactions modulated by electrostatic repulsion and weak attractive interaction. Any change in solvent condition that can change any of these factors can dramatically change the solution structure and the light scattering of the protein solution.

For long time it was generally accepted that aggregation of lens proteins, as a result of drastic changes in protein structure, is responsible for the increase of light scattering in older lenses. This can evolve to the dramatic effect of cataract. The important role of the major α-crystallin protein in the formation of the large scattering units was taken for granted (Spector and Katz, 1965; Harding and Dilley, 1976; Siezen et al., 1979). Recently, it has been shown that some types of cataract, such as cortical cataracts, are associated with disturbances in local ion concentration, which results from malfunctioning of membrane ion channels (Duncan et al., 1989). In light of our results on the interaction potential of α-crystallin, it is possible that small changes in the ionic conditions can drastically change the interparticle interaction and consequently the cytoplasm solution structure and light scattering.

MATERIALS AND METHODS

Preparation of calf lens cytoplasm and α-crystallin

The lenses of 6-month-old (±2 weeks) calves were obtained from a slaughterhouse within 3 h after slaughtering and were subsequently stored at 4°C. The lens capsule was removed and the lenses were mixed with a sixfold quantity of buffer (containing 10 mM Hepes, 120 mM KCl, 25 mM NaCl, 0.02% NaN_3, pH 7.0) and gently stirred at 4°C for 20 min. In this way only the outer cortical cells were dissolved. This suspension was centrifuged at 12,000 *g* for 30 min to remove the insoluble material. The concentration of water-soluble supernatant was determined from the refractive index of the solution at 632.8 nm according to the experimental relation (Delaye and Gromiec, 1983)

$$n = 1.3336 + 0.182 \cdot c \qquad (2)$$

where c is the concentration in percent.

About 20 ml of cortical protein solution, dissolved in the above mentioned buffer (containing about 2000 $A^{1\,cm}_{280\,nm}$ units), was loaded on a Bio-Gel A-5m column (ϕ 5 × 85 cm, Bio-Rad, Richmond, CA) at 4°C and the eluent was collected in 15-ml fractions. The top fractions of the low molecular mass α-crystallin elution zone (Andries et al., 1982) were collected and eventually concentrated by using an Amicon concentration cell (model 52) and an XM-100 filter system (Amicon Corp., Lexington, MA).

After concentrating the α-crystallin solution, the solution was centrifuged at 12,000 *g* in a JA20 Beckman rotor (Beckman Instruments, Inc, Palo Alto, CA) for 30 min to remove the dust particles and large aggregates of α-crystallin resulting from the concentration step. The centrifuged α-crystallin solution (±10 ml) was then extensively dialyzed against the appropriate buffer solution. For that purpose, the solution was put in a visking dialysis bag (Medicell International Ltd, London, UK). The dialysis bag was put into a dialysis tube (ϕ 10 × 40 cm containing ~500 ml dialysis buffer) and slowly turned around in order to shake the dialysis tube. To make sure that the ionic strength of the α-crystallin solution in the dialysis bag was in equilibrium with that of the outside buffer, the α-crystallin solution was stirred for at least 24 h, and every 6 to 8 h the outside buffer was renewed. For the light scattering measurements, we prepared the α-crystallin in five different ionic strength buffers. The ionic strength of buffers ranged from very low (0.0022 M) to high (0.5822 M). The composition of the five buffers is shown in Table 1. For the measurement of different α-crystallin concentrations, the dialysis buffer was added to dilute the α-crystallin solution. The exact concentration of α-crystallin was calculated from the measurement of the $A^{1\,cm}_{280\,nm}$ and accepting the $A^{1\%,\,1\,cm}_{280\,nm}$ value of 8.1 (Delaye and Gromiec, 1983).

Light scattering measurements: experimental procedures

The light scattered by α-crystallin solutions was measured using a light scattering instrument in a thermostated room. Since dust particles will influence the scattering of light to a great extent, special attention was paid to this point. The cylindrical glass scattering cells, stored in an ethanol-HCl mixture, were washed with distilled water and further cleaned by flushing the surface with condensing acetone vapor in an apparatus specially designed for that purpose (Tabor, 1972). For diluting the protein solution, a filtered buffer was used (MF-Millipore filter GS 0.45 μm). A centrifugation step of the filled scattering cell up to 6000 rpm in a specially constructed adapter for a JS13 Beckman rotor for 1 h removed by sedimentation the dust particles from the scattering volume.

A beam of light with a wavelength of λ = 488 nm and 30 mW from an argon ion laser (model 2016, Spectra-physics Inc, Mountain View, CA) was focused in the cell. The scattered light was detected with a photomultiplier (FW130, Electro-Optical Products Division, International Telephone & Telegraph, Fort Wayne, IN). The light intensity scattered by the solutions was measured at different scattering angles ranging from 50° to 130° in steps of 10°. To relate the intensity I_p, scattered by the α-crystallin solution, to the incident intensity, I_0, toluene was used as a standard scatterer. All results from light scattering were corrected for dark current.

From the light scattered by the α-crystallin solution, the Rayleigh ratio $R_p(\theta)$ was calculated using the following relation

$$R_p(\theta) = \frac{I_p(\theta) - I_b(\theta)}{I_t(\theta)} \times R_t(\theta) \times \left(\frac{n_p}{n_t}\right)^2 \qquad (3)$$

TABLE 1 Composition of five different ionic strength buffers and some of their properties

Buffer	Composition	Ω	κ	κ^{-1}
		(M)	(nm^{-1})	(nm)
1	10 mM Hepes, 0.02% NaN_3, pH 7.0	0.0022	0.153	6.504
2	10 mM Hepes, 5 mM KCl, 1 mM NaCl, 0.02% NaN_3, pH 7.0	0.0082	0.296	3.369
3	10 mM Hepes, 25 mM KCl, 5 mM NaCl, 0.02% NaN_3, pH 7.0	0.0322	0.578	1.727
4	10 mM Hepes, 120 mM KCl, 25 mM NaCl, 0.02% NaN_3, pH 7.0	0.1472	1.257	0.795
5	10 mM Hepes, 480 mM KCl, 100 mM NaCl, 0.02% NaN_3, pH 7.0	0.5822	2.496	0.401

Ω is the ionic strength: $\Omega = 0.5 \cdot \sum M_i Z_i^2$, where Z_i the ionic valence and M_i the molar concentration of the ion i. κ and κ^{-1} are the Debye constant and Debye length.

where $I_p(\theta)$ is the intensity scattered by the protein solution at an angle θ; $I_t(\theta)$ is the intensity scattered by the reference solvent at an angle θ; $I_b(\theta)$ is the background stray light and solvent contribution; n_p,n_r is the index of refraction of the solution and reference solvent, respectively; and $R_t(\theta)$ is the Rayleigh ratio of the reference solvent toluene. For the Rayleigh ratio of toluene $R_t(\theta)$, we have used a value of $39.6\times10^{-1}\text{m}^{-1}$ (Bender et al., 1986).

The light scattered by a diluted solution of particles is commonly represented by the following equation

$$\frac{Kc}{R_p(k)} = \frac{1}{P(k)} \cdot \frac{1}{\langle M\rangle_w}(1 + K_I\phi) \tag{4}$$

where K is $4\pi^2n^2(dn/dc)^2/N_A\lambda_0^4$: n is the refractive index of reference solvent toluene $n = 1.507$; dn/dc is the refractive index increment of the α-crystallin protein solution 0.195 ml · g^{-1} (Andries et al., 1982); λ_0 is the wavelength of the laser beam in vacuum, $\lambda_0 = 488$ nm; N_A is Avogadro's number; k is the scattering vector $[4\pi n_0/\lambda_0] \cdot \sin(\theta/2)$; c is the concentration of particles in mg/ml; $P(k)$ is the particle form factor; $\langle M\rangle_w$ is the weight-average molar mass of the particles in solution; K_I is the static coefficient; and ϕ is the volume fraction of particles $\phi = c\nu$, where ν is the specific hydrodynamic volume of the solute particles. As the particles are small relative to the wavelength of the incident beam, $P(k) = 1$.

The above theories have been developed for monodisperse solutions and they have to be adjusted if considering a polydisperse particle solution. α-Crystallin is polydisperse (Schurtenberger and Augusteyn, 1991), and this will affect the results in various ways. The polydispersity effects can easily be described in the absence of interparticle interactions. Assuming that the size distribution is log-normal with a maximum at diameter d_0 and variance δ, we calculate that the effective molar mass M is related to the molar mass M_0 of the most probable particle by the following expression (Licinio and Delaye, 1988)

$$M = M_0(1 + \delta^2)^{27/2} \tag{5}$$

where M is the molar mass deduced from the extrapolation to $c = 0$ of $Kc/R_p(k)$; M_0 is the molar mass corresponding to a diameter d_0; and δ is the variance that quantifies the polydispersity.

The effective hydrodynamic radius a roughly corresponds to a sixth-order moment of the size distribution divided by a fifth-order moment. For the same log-normal distribution we can calculate

$$a = a_0(1 + \delta^2)^{11/2} \tag{6}$$

where a is the hydrodynamic radius deduced from extrapolation to $c = 0$ of the diffusion coefficient D, and a_0 is the hydrodynamic radius corresponding to diffusion coefficient D_0, the diffusion coefficient of the most probable particle.

The average volume $\pi d^3/6$ is related to the volume of the most probable particle (with diameter d_0) by the expression

$$d^3 = d_0^3(1 + \delta^2)^{9/2} \tag{7}$$

where d is the particle hydrodynamic diameter.

After considering the polydispersity and taking into account the effect of the molar mass M and the hydrodynamic radius a, the specific volume of a polydisperse solution of particles can be calculated in the following way:

$$\frac{\phi}{c} = \frac{\pi \cdot N_A \cdot d_0^3}{6 \cdot M_0} = \frac{\pi \cdot N_A \cdot d^3}{6 \cdot M}(1 + \delta^2)^9. \tag{8}$$

K_I, the static coefficient, derived from the light scattering experiment using Eq. 4, is dependent on the value of $\phi = c\nu$. When considering the polydispersity in the results of light scattering by α-crystallin proteins in different ionic strength, we have to known δ. This can be calculated from the experimental molar mass M and hydrodynamic radius a (see Table 2) and the values of $M_0 = 600{,}000$ and $a_0 = 8.5$ nm (Coopman et al., 1984; Tardieu et al., 1986; Schurterberger and Augusteyn, 1991; Augusteyn et al., 1992). We obtained a value $\delta = 0.14 \pm 0.03$, which results in a correction of factor of 1.19 for the hydrodynamic volume ϕ. This resulted in the corrected values K_I for the static factor.

TABLE 2 Experimental molar mass M, hydrodynamic radius a, hydrodynamic volume ν, and the static coefficient K_I of the α crystallin protein solutions

Ω	κ^{-1}	a	ν	Mole mass	K_I
(M)	(nm)	(nm)	(cm^3)	(g/mol)	
0.0022	6.504	9.39	2.62	798,600 ± 8,352	24.59 ± 0.43
0.0082	3.369	9.77	2.75	839,100 ± 37,947	16.04 ± 1.23
0.0322	1.727	9.59	2.76	803,600 ± 11,292	10.45 ± 0.35
0.1472	0.795	9.27	2.68	758,600 ± 25,069	8.54 ± 0.23
0.5822	0.401	9.23	2.64	753,700 ± 34,404	7.79 ± 0.30

Ionic strength buffers ranged from 0.0022 to 0.5822 M. The range of the electrostatic interactions is quantified by the Debye-Hückel length κ^{-1}.

Diffusion coefficient measurements

Photon correlation spectroscopy has been used for the determination of the diffusion coefficient of the α-crystallin protein in solvents with different ionic strengths. Light scattered by the solutions containing the α-crystallin particle was detected with an ITT FW 130 photomultiplier and the photocurrent output of the photomultiplier was analyzed using a Brookhaven BI-8000 AT correlator. The setup was installed in a thermostated room and the temperature was monitored directly in the scattering cell.

Solutions containing crystallin proteins with hydrodynamic radius 8.5 nm and larger and at concentrations of 0.5 mg/ml or higher can be studied easily by photon count autocorrelation spectroscopy if the necessary precautions are taken to obtain optimal conditions (Andries et al., 1983). The conditions were set to obtain a signal to noise (S/N) ratio of at least 0.35. The S/N value is defined from the second-order correlation function $g^2(t)$ or scattered intensity $I(t)$

$$\text{S/N} = \frac{g^2\ (t = 0)}{g^2\ (t = \text{infinite})} - 1 = \frac{\langle I^2\rangle}{\langle I\rangle^2} - 1. \tag{9}$$

To obtain these conditions, the solutions have to be dust-free, the optical lining of the light beam has to be optimal, and the primary intensity of the intensity stabilized argon ion laser has to be adjusted properly. A laser intensity that is too high can heat the solution and the toluene bath surrounding the scattering cell. Furthermore, increased uncorrelated reflections of the light beam increased the noise. The quality of our setup was routinely checked by measurements at scattering angles of 50°, 90°, and 130°.

For a diluted homogeneous solution containing spherical particles, which are small compared with the wavelength of the light, the intensity correlation function measured with a homodyne correlation setup becomes, in its normalized form,

$$g^2(t) = 1 + \gamma \cdot \exp(-2 \cdot D \cdot k^2 \cdot i \cdot \tau), \tag{10}$$

where γ is the an experimental constant that depends on the correlation volume and the quality of the optical setup. This parameter γ equals the S/N factor defined above, so we have always tried to obtain a value of about 0.35; D is the diffusion coefficient of the particles; τ is the sample time; and i is the channel number.

Although we expect a monodisperse crystallin protein solution, we have routinely used three ways of analyzing the experimental intensity correlation functions: the cumulant analysis method (Koppel, 1972), a double exponential fit method, and the exponential sampling method (Ostrowsky et al., 1981). The concentration dependence of the diffusion coefficient of α-crystallin can be presented in the following manner:

$$D = D_0(1 + K_D\phi) \tag{11}$$

where D_0 is the diffusion coefficient value at the concentration $c = 0$, and K_D is the parameter which describes the concentration dependence of the diffusion coefficient when using the volume fraction ϕ as concentration parameter.

In the limit of zero concentration and for a monodisperse solution of spherical particles, the hydrodynamic radius of α-crystallin particle a_h can be derived from the free particle diffusion coefficient D_0 by using the Stokes-Einstein equation.

Light scattering: theoretical relations

Generally we can write for the Rayleigh ratio $R(k)$ of a solution of interacting particles

$$\frac{K_C}{R_p(k)} = \frac{1}{P(k) \cdot \langle M \rangle_w \cdot S(k)} \tag{12}$$

where $S(k)$ is the structure factor. This is the ratio of the actual scattered intensity at any particular scattering vector to that intensity which would be scattered by an identical collection of particles that do not interact. The structure factor $S(k)$ is related to the radial distribution function $g(r)$ in the following way:

$$S(k) = 1 + 4\pi c k^{-1} \int [g(r) - 1] \cdot r \cdot \sin(kr) \cdot dr \tag{13}$$

where $g(r)$ is the probability of finding two particles at a distance r from each other.

This radial distribution function $g(r)$ can be calculated if the particle pair interaction $V(r)$ is known. Various approximations have now been used to derive $g(r)$. For a diluted solution of small particles ($P(k) = 1$), Eq. 12 reduces to Eq. 4.

In the diluted gas approximation and using the one component macrofluid liquid model, the following expression has been obtained for the static coefficient K_I (Corti and Degiorgio, 1981):

$$K_I = 8 + 24 \int_0^\infty dx(1 + x)^2(1 - e^{-V(x)/(K_B T)}) \tag{14}$$

where 8 is the hard-sphere contribution; x is $(R - 2a)/2a$ (R, the distance between the centers of the two particles, and a, the radius of the spherical particle); and $V(x)$ is the interaction potential between a pair of spherical particles.

The interaction potential $V(x)$ according to the Derjaguin-Landau-Verwey-Overbeek theory (Verwey and Overbeek, 1948) is the sum of two contributions, where V_R is a repulsive interaction and V_A is an attractive interaction:

$$V(x) = V_R + V_A. \tag{15}$$

The repulsive interaction V_R depends on 1) the size of the spherical particle, 2) the number of charges on the surface of the particle, and 3) the range of interaction.

The protein particles, which have charges on their surface, are dissolved in an electrolyte solution. The counterions tend to cluster around the central opposite charged proteins. The influence of the counterion distribution is expressed by the thickness of the ion atmosphere; this thickness around the charged macromolecule is related to the quantity (κ^{-1}) called the Debye radius. κ is given by:

$$\kappa = \left(\frac{8\pi N_A e^2 \rho}{1000 \epsilon K_B T} \cdot \Omega\right)^{1/2} \tag{16}$$

where ρ is the solvent density; e is the electron charge 4.803×10^{-10} esu; ϵ is the solvent dielectric constant; Ω is the ionic strength $\Omega = 0.5 \times \sum M_i Z_i^2$; M_i is the molar concentration of ion i, and Z_i its charge.

When the ions are treated as point charges obeying the Poisson-Boltzmann equation, the layer of ions is divided into two parts: the Stern layer, which is a thin inner region, and the Gouy layer, which is the diffuse outer region. The long range repulsion is determined by the potential of the diffuse layer.

As it is not possible to obtain an analytical solution of the Poisson-Boltzmann equation in most conditions, numerical solutions have been tried. Then analytical expressions have been proposed which approach these numerical solutions to a reasonable limit.

A successful trial has been made by Ohshima and co-workers (Oshima et al., 1982), which results in an expression for the interaction potential V_R by expressing the surface charge density/surface potential relationship and the double-layer potential distribution for a spherical particle. Their expressions yield a solution for ψ, which is correct to first order in $(\kappa a)^{-1}$ for any value of the surface potential and results in a very good approximation for the second term in $(\kappa a)^{-1}$ for a surface potential values $\psi_s < 5$.

The dimensionless surface charge density J is given by

$$J = \frac{q \cdot e^2}{4 \cdot \pi \cdot a^2 \cdot \kappa \cdot \epsilon \cdot \epsilon_0 \cdot K_B \cdot T} \tag{17}$$

where q is the particle charge number.

The surface charge density J can be expressed as a function of the surface potential ψ_s.

$$J = 2 \cdot \sinh\left(\frac{y_s}{2}\right) + \frac{4}{\kappa a} \tanh\left(\frac{y_s}{4}\right) \tag{18}$$

where y the reduced surface potential ($e\psi_s/K_B T$).

The reduced surface potential y_s of a particle in solution depends on the particle charge, the ionic strength, and the particle radius. The potential distribution around a spherical particle can be expressed in following way:

$$Y(s) = 2 \cdot \ln\left[\left(\frac{1 + Cs}{1 - Cs}\right) \times \frac{1 + Cs/(2\kappa a + 1)}{1 - Cs/(2\kappa a + 1)}\right] \tag{19}$$

where $s = (\kappa a/\kappa r)\exp(-\kappa r + \kappa a)$ and r is the distance from the particle surface. The parameter C in Eq. 19 is equal to

$$C = \tanh\left(\frac{Y_s}{4}\right)\left[\frac{(1 + \kappa a)/(\kappa a + 1)}{1 + \left\{1 - \frac{2\kappa a + 1}{(\kappa a + 1)^2} \tanh^2\left(\frac{Y_s}{4}\right)\right\}^{1/2}}\right] \tag{20}$$

To obtain the interaction energy of two spheres of radii a_1 and a_2 atlarger distances between their centers, the potentials around each separated sphere are added in a linear way; this yields an expression for the potential and therefore also for the interaction energy, correct to leading order in the separation distance. Under these conditions, the interaction potential V_R is given by

$$V_R = \frac{4 \cdot \pi \cdot \epsilon_0 \cdot \epsilon (K_B T/e)^2 \cdot a \cdot Y_1 \cdot Y_2 \cdot \exp(-2a\kappa x)}{2x + 2} \tag{21}$$

where Y_1, Y_2 are the asymptotic constants; when the radius $a_1 = a_2$, $Y_1 = Y_2$.

In Eq. 21, Y_1 and Y_2 are given by

$$Y = 8 \cdot \tanh\left(\frac{y_s}{4}\right) \frac{1}{1 + \left(1 - \frac{2\kappa a + 1}{(\kappa a + 1)^2} \cdot \tanh^2\left(\frac{y_s}{4}\right)\right)^{1/2}} \tag{22}$$

where y_s is the surface potential; its value can be obtained from Eq. 18 when the surface charge density J is known from Eq. 17.

The expression for the attractive London–van der Waals potential V_A, derived by Hamaker for the case of two spherical particles, is given by (Hamaker, 1937)

$$V_A = -\left(\frac{A}{12}\right)\left[\frac{1}{(x^2 + 2x)} + \frac{1}{x^2 + 2x + 1} + 2 \ln \frac{(x^2 + 2x)}{(x^2 + 2x + 1)}\right] \tag{23}$$

where A is the Hamaker constant and x is the reduced interparticle distance: $x = (R - 2a)/2a$, where a is the particle radius and R is the distance between two particle centers.

This equation does not take into account retardation effects and therefore is not valid for large values of x.

RESULTS

Light scattering of α-crystallin solutions

The light scattering of calf lens α-crystallin solutions was measured in five different ionic strength buffers. The ratio of I_p, the net scattered intensity by the α-crystallin solutions, to I_t, the intensity scattered by toluene, ranged from 10 to 450 as related to the concentration of α-crystallin and the ionic strength. At the different scattered angles θ from 50° to 130°, almost identical results were obtained. This is expected for the α-crystallin particles, where the largest dimension is smaller than λ/20 (Tanford, 1961). It also means that the sample solutions are free from large dust particles. All measurements were performed with the same power of the incident laser beam.

The scattered intensities, measured in five different ionic strength buffers as a function of the α-crystallin concentration, are plotted in Figure 1. The results indicate that at low concentration, the positions of the scatterers are not correlated and the intensities from the various scatterers are additive.

The ionic strength and the protein concentration do influence the interaction between the protein molecules. When the concentration increases, the interaction between the scattering particles becomes more important as the distance between the scatterers is comparable with their interaction range so that some spatial correlation appears, and this disturbs the linear increase of I_p. At lower ionic strength, the electrostatic interaction range is more important, so the spatial correlation will start to happen at lower protein concentration.

To characterize further the static light scattering of α-crystallin solutions, the data of Figure 1 are plotted according to the Eq. 4. From the linear part of the curves of Figure 1, the molar mass has been obtained of the α-crystallin protein in different ionic strength buffers on extrapolating the quantity $K'c/(I_p/I_t)$ to $c = 0$. These values are listed in Table 2. A mean value of (790,000 ± 35,000) g/mole results from these data; this agrees with the values from literature (Andries et al., 1982).

Diffusion coefficient measurement of α-crystallin solutions

In the photon correlation spectroscopy experiments, the normalized autocorrelation function of the scattered light was analyzed to determine the diffusion coefficient of the α-crystallin protein particle as function of the concentration of the α-crystallin protein in five different ionic strength solvents. To estimate some parameters of the α-crystallin particle from the experimental diffusion coefficients in the different ionic strengths, and to allow a straightforward comparison of the measurements of photon correlation spectroscopy to the results of light scattering, we have used identical solvent conditions and the same concentration range of the α-crystallin protein. For this purpose, the same α-crystallin solutions have been used to measure the light scattering intensity first and then the photon correlation spectrum.

The representative plots of the experimental diffusion coefficient, D_z, of the α-crystallin protein as the function of protein concentration, at different ionic strengths, indicate that the concentration dependence of D_z varies strongly with the ionic strength of the solvent: the lower the ionic strength, the larger the concentration dependence. There is, however, a common intercept D_0 when extrapolating the diffusion coefficient D_z to the concentration of α-crystallin $c = 0$ for all

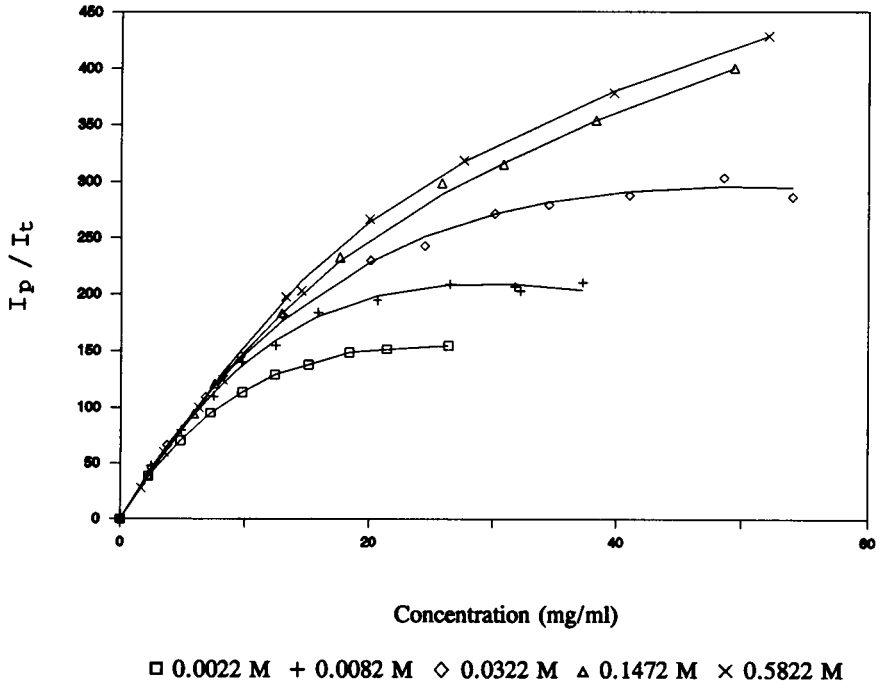

FIGURE 1 Scattered intensity relative to toluene by α-crystallin solutions in five different ionic strength buffers as a function of the concentration of the α-crystallin protein.

ionic strengths. This means that there is no important change in the hydrodynamic structure of the α-crystallin going from a low (0.0022) to a high (0.5822) ionic strength buffer.

The hydrodynamic specific volume that can be calculated from the molar mass, obtained from light scattering measurements and hydrodynamic radius a_h, can also be considered as independent from the ionic strength in the range of 0.0022 to 0.5822 M.

Hydrodynamic parameters of α-crystallin

Table 2 gives experimental data from light scattering and photon correlation spectroscopy measurements of low concentration α-crystallin solutions in different ionic strength buffers. The values were obtained from extrapolating the experimental data to a concentration 0 or from the limiting slope of experimental curves at zero concentration, independent of any model structure.

At all solvent conditions, α-crystallin behaves as a noncompact aggregate: its hydrodynamic volume is a factor (2.7 ± 0.1) greater than the equivalent hard sphere of the same molar mass. As the static coefficient K_I deviates from the theoretical value $K_I = 8$ for hard-sphere particles in any solvent conditions, we have to take into consideration both electrostatic repulsive and attractive interactions. The former are most important at low ionic strength, whereas at high ionic strength, mainly the attractive interaction contributes to K_I.

The α-crystallin proteins are dissolved in different ionic strength buffers. There are charged groups on the α-crystallin protein. For the solution behavior, the charges on the particle surface are important. According to the Debye-Hückel theory, the counterions tend to cluster around the opposite charge on the protein surface while they are attracted there by the favorable electrostatic interaction potential. This accumulation is opposed by the randomizing thermal forces that cause particles to move away from regions of high concentration. A quantitative description of the counterion distribution is given by the thickness of the ion atmosphere defined by the quantity (κ^{-1}). The Debye radius (κ^{-1}) of the five different ionic strength solvents used in our experiments is given in Table 1. When the ionic strength Ω increases, the Debye radius κ^{-1} decreases. In the high ionic strength buffer, the Debye radius (κ^{-1}) is small compared with the radius a of the protein molecules; this allows us to consider the α-crystallin protein in these conditions almost as a hard sphere. This is confirmed by the fact that the K_I value is close to 8. For the lower ionic strength conditions, K_I is higher than 8. This is due to the fact that at least two factors are involved in the particle interaction and light scattering behavior; namely, the excluded volume effect of the hard spheres and the electrostatic interaction between the charged particles, which becomes more important at low ionic strength.

Repulsive interactions

The experimental K_I values in buffer conditions 1 to 4 and the changes in K_I as a function of ionic strength clearly indicate that the α-crystallin proteins repulse each other, and that this repulsion force depends on the ionic strength. We have corrected the experimental K_I for the attractive interaction by setting its value at high ionic strength, where all electrostatic interactions should be almost completely screened off, equal to the hard sphere value 8. For the other solvent conditions, we have applied the same correction.

We have used the procedure, as proposed by Corti and Degiorgio (1981), to take into consideration an explicit expression for the interaction potential $V(x)$, and we have applied this expression for the calculation of K_I. First we used only the repulsive contribution to $V(x)$. The Oshima expression V_R uses three parameters: the charge q, the radius of the sphere a, and the Debye constant κ (Eq. 21).

At some defined ionic strength so that κ is fixed and for a solution of spherical particles with known radius a, K_I depends on one parameter, the charge q. By fitting the theoretical expression of K_I to the experimental values, it is possible to estimate the charge q of the particles. The results are given in Table 3.

It is striking that the charge q of the proteins does change from 18 at an ionic strength of O.0022 M to 50 at an ionic strength of 0.1472 M. This change is related to the change of the dissociation constant K_{DIS} of the dissociable groups of the side chains of the amino acids glu, asp, his, lys, arg, and cys on changing the ionic strength. The influence of the ionic strength on the dissociation constant K_{DIS} and pK is quantified by the following expression (Edsall and Wyman, 1958)

$$HB^q \rightleftarrows H^+ + B^{q-1}$$

$$pK' = pK_0 + \log\left(\frac{f_{B^{q-1}}}{f_{HB^q}}\right) \tag{24}$$

$$\log f_{HB^q} = \frac{0.5 \cdot q^2 \cdot \sqrt{\Omega}}{1 + K_1 \cdot K_2 \cdot \sqrt{\Omega}} - K_3 \cdot \Omega$$

where pK_0 is the intrinsic dissociation constant, pK′ is the apparent dissociation constant, HB^q is the acid form, B^{q-1} is the basic form, q is the electric charge, f is the activity coefficient, Ω is the ionic strength, K_1 and K_2 are constants, and K_3 is the interaction constant.

TABLE 3 Estimated charge q of the particles in four different ionic strength buffers

Ω	κa	K_I	q from K_I
(M)			
0.002	1.44	24.80 ± 0.43	18 ± 1
0.0082	2.90	16.25 ± 1.23	33 ± 4
0.0322	5.55	10.66 ± 0.35	40 ± 4
0.1472	11.73	8.75 ± 0.23	50 ± 5
0.5822	23.04	8.00	

Data were obtained by fitting the theoretical expression of K_I to the experimental values corrected for the attractive interaction.

If the charge q is positive, an increase in ionic strength will increase the pK; if q is 0 or negative, the change will be in the other direction. For α-crystallin, which contains more A (acidic) peptides than B (basic) peptides so that the isoelectric point is below pH 7.0 (Bloemendal, 1981), it can be expected that the isoelectric pH will decrease on increasing the ionic strength. Therefore at high ionic strength, pH 7 will be further away from the isoelectric pH than at low ionic strength. It can be expected therefore that at pH 7, α-crystallin at high ionic strength has more charges exposed to the solvent than at lower ionic strength. This explains the results shown in Table 3.

This behavior is confirmed by potentiometric titration studies of α-crystallin at high (Ω = 0.145 M) and low ionic strength (0.0025 M) as shown in Figure 2. This figure gives the moles of base or of acid added per mole of 20-kDa peptide to reach a defined pH. To have a quantitative idea about the absolute number of charges on each 20-kDa peptide, which are accessible from the solvent, we have to know the zero point or the isoelectric pH.

Many methods can be used to determine the isoelectric point. They are based on two principles: on movement in an electric field or on charge interaction. At the isoelectric pH, either the proteins do not move any more in an electric field or they do not show any charge interaction. However, both of these methods can only be used at low ionic strength. At high ionic strength, the solubility method can be used. This method is based on the idea that at the isoelectric pH, the solubility of a protein is minimal; one has to be lucky that this minimal solubility can be reached within available experimental conditions.

Figure 3 shows the solubility curve of solutions of α-crystallin at low (0.0025 M) and high (0.145 M) ionic strength. The solubility has been monitored by measuring the absorbance at 400 nm; this wavelength is just outside the protein ultraviolet absorption range. An increase in absorption at 400 nm indicates an increase in light scattering, which is related to an increase in aggregation. These aggregates are formed close and at the isoelectric pH; the curve absorbance at 400 nm versus pH is symmetrical, which indicates that the aggregation phenomenon is reversible. This finding improves the theoretical basis of this method to determine the isoelectric pH. Our results also showed that this method can be used in a broad range of ionic strengths for this type of protein.

From this figure we can conclude that at Ω = 0.145 M the isoelectric pH is 4.45, and at Ω = 0.0025 it is 5.05. This coincides with the fact that α-crystallin has an isoelectric pH below 7.0. We also can calculate the number of charges each 20-kDa peptide has at pH 7.0. At high ionic strength (0.145 M), this turns out to be −9.25 units; if we accept a molar mass of 800,000 g/mole for α-crystallin, we can conclude that this oligomeric protein has 370 minus charges on its surface, available for the solvent. At low ionic strength, this turns out to be 190 minus charges. These values are much higher, but have about the same ratio, as the charges we could conclude from our light scattering measurements. This can be explained by the fact that the two sets of values are at different levels.

Potentiometric titrations give us the total number of charges that can be reached from the solvent; these charges are distributed on the surface but can also be situated in crevices of the protein surface. The light scattering data refer to the long range electrostatic repulsion between the diffuse outer layer around the protein particles (Verwey and Overbeek, 1948).

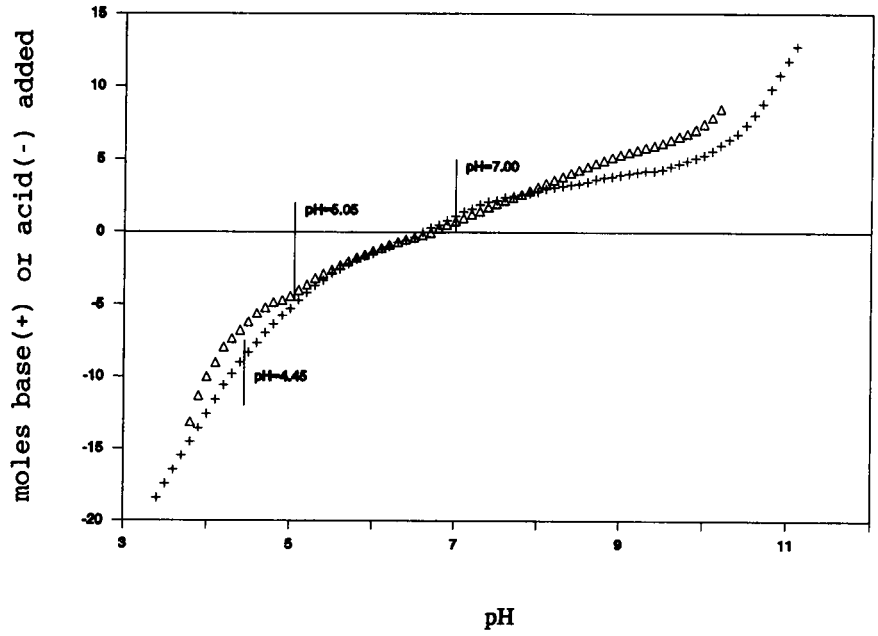

FIGURE 2 Moles of base or acid added per mole 20-kDa peptide as a function of pH. The solvent contribution has been subtracted.

+: at high ionic strength (0.145 M) ▵: at low ionic strength (0.0025 M)

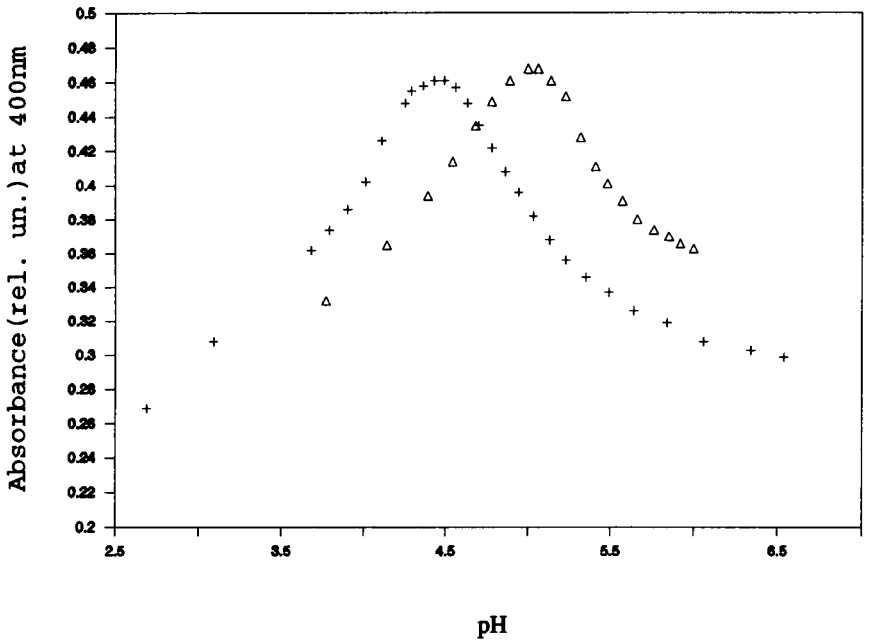

FIGURE 3 Solubility of α-crystallin at high and low ionic strength as function of pH.

+: at high ionic strength (0.145 M) ▵: at low ionic strength (0.0025 M).

For a control on our model and the parameters that define this model such as size of spherical particles and charge distribution, we have calculated the structure factor $S(k, c)$. This static structure factor accounts for the spatial distribution of the particles in solution.

We have calculated the function $S(0, \phi)$ using the renormalized mean spherical approximation as proposed by Hayter and co-workers (Hayter and Penfold, 1981; Hansen and Hayter, 1982). Table 4 shows that at low volume fraction, where the structure factor can be considered as a linear function of ϕ, the initial slope of the theoretical structure factor agrees with our experimental K_I values at a wide range of ionic strengths (0.0022 to 0.1472 M).

TABLE 4 Initial slope of the α-crystallin structure factor in four ionic strengths

Ω	Charge q (used for RMSA calculations)	$S(0, \phi)$ (from RMSA calculations)	$1/(1 + K_{I,exp} \cdot \Phi)$ at $\phi = 0.01$
(M)			
0.0022	18	0.7464	0.8013
0.0082	33	0.8311	0.8602
0.0322	41	0.8932	0.9037
0.1472	50	0.9164	0.9195

The structure factor $S(0, \phi)$ was calculated using the renormalized mean spherical approximation (RMSA) methods using the q values from Table 3. q values resulted from the diluted gas approximation accepting a electrostatic repulsion and using the Ohshima expression for the interaction potential. A radius of 9.4 nm was accepted for the spherical particle; experimental K_I values are taken from Table 3.

Attractive and repulsive interactions

It is possible to take into account the attractive and repulsive interaction between α-crystallin particles by taking into account the contribution of a repulsive interaction V_R and an attractive part V_A to the interaction potential $V(x)$. We can calculate $V(x) = V_R + V_A$; for V_R we use the Ohshima expression (Eq. 21) and for V_A we use the London–Van der Waals expression (Eq. 23).

By introducing these expressions in Eq. 14 we are left with expressions for K_I that depend on two parameters: the number of charges q and the value of the Hamaker constant A. For every ionic strength, there is a continuous set of the two parameters that result in theoretical values of the parameter K_I which fit the experimental values. This is illustrated in Figure 4, which gives the sets of the Hamaker constant A and electric charge number q values that fit the experimental K_I values at the ionic strengths 0.0022 to 0.5822 M.

At lower ionic strength (Ω = 0.0022 M), where the repulsive interaction potential is quite high, the choice of the value for the Hamaker constant A hardly influences the electrostatic repulsion potential. A Hamaker constant of 0 requires a charge q of 17.85 to fit the experimental static coefficient K_I of 24.6, whereas a slight increase of the charge value to 20 requires a dramatic increase of A to 0.226.

At high ionic strength, the interaction parameter K_I mainly depends on the Hamaker constant and is much less dependent on the electric repulsion and the charge q of the spherical particles. Figure 4 also allows an estimate of the Hamaker constant A of the α-crystallin particle. Indeed, it is reasonable to accept that A does not depend on the ionic

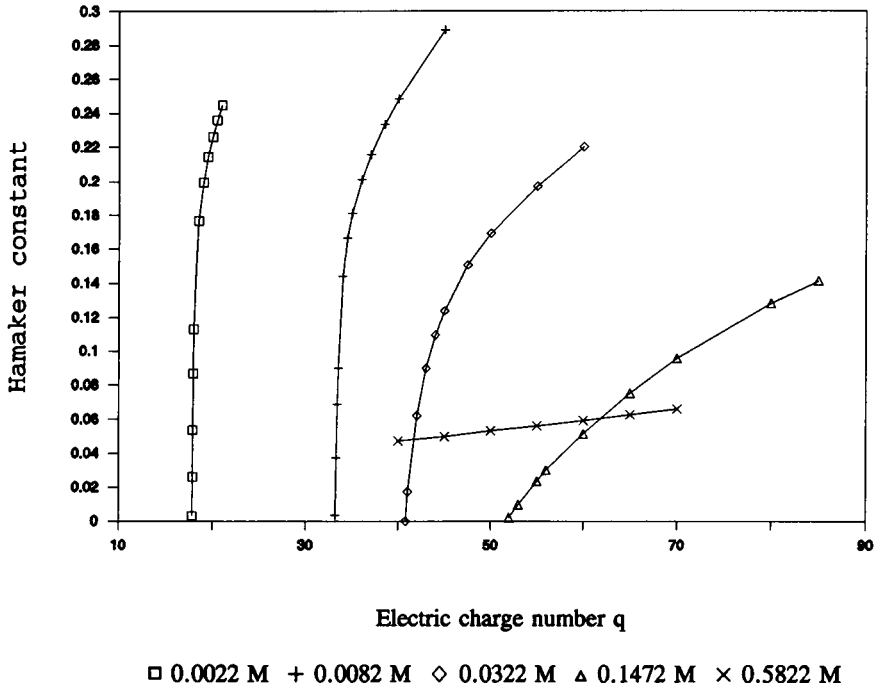

FIGURE 4 Sets of the Hamaker constant A and electric charge number q, which fit the experimental K_I in the five different ionic strength buffers.

strength; it is also reasonable to accept that at high ionic strength the charge q of the α-crystallin particle will only be slightly dependent on the ionic strength. Therefore, a good estimate for A and q at higher ionic strength can be obtained from the intercept of the two q, A curves at ionic strengths $\Omega = 0.5822$ M and $\Omega = 0.1472$ M. This results in Hamaker constant $A = (0.06 \pm 0.01)K_BT$. The presence of an attractive component in the interaction potential $V(x)$ is also clearly evident in the results of light scattering in a volume fraction range 0 to 0.60 at an ionic strength of 0.1472 M (see Fig. 5). For the structure factor $S(0, \phi)$ of a solution of hard spheres, we have used the Carnahan and Starling formula (Delaye and Tardieu, 1983). For the calculation of the structure factor of a solution of hard spheres showing electrostatic repulsion, we have used the rescaled mean spherical approximation method and the procedure of Hayter and Penfold (1981). For characterizing the α-crystallin particles, we have accepted a hard-

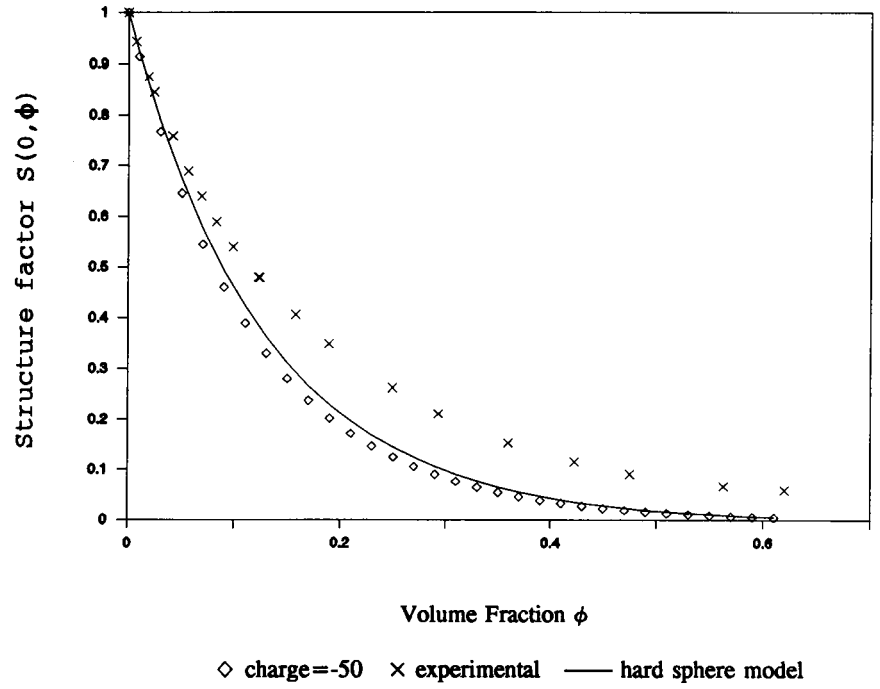

FIGURE 5 Structure factor $S(0, \phi)$ calculated from light scattering measurements of α-crystallin solutions at an ionic strength of 0.1472 M, as compared with theoretical values of $S(0, \phi)$ for a solution of hard spheres or a solution of hard spheres showing electrostatic repulsion.

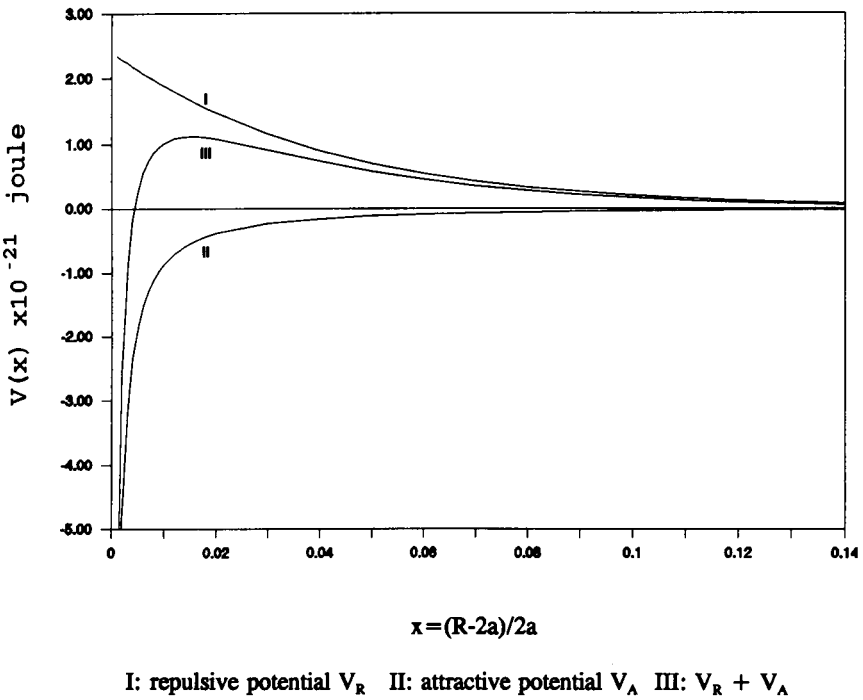

FIGURE 6 Pair interaction potential $V(x) = V_R + V_A$ as a function of the reduced-normalized distance x at the conditions of a spherical particle with radius a = 9.4 nm at an ionic strength of 0.1472 M, a charge number q = −50, and a Hamaker constant $A = 0.06\ K_BT$.

sphere radius of 9.4 nm and a surface charge of −50, and we have used the Ohshima expression (Eq. 21) for describing the electrostatic interaction potential.

A comparison with the experimental curve indicates that we have to include an attractive component in the interaction potential $V(x)$ to obtain a theoretical structure factor that covers the experimental function $S(0, \phi)$.

DISCUSSION

α-Crystallin solutions have extensively been studied by light scattering (Andries and Clauwaert, 1985; Tardieu et al., 1986), photon correlation spectroscopy (Licinio and Delaye, 1988), x-ray scattering (Tardieu et al., 1987), osmotic pressure measurements (Vérétout and Tardieu, 1989), or a combination of these techniques (Vérétout et al., 1989).

Most of these studies were performed at concentrated solutions. This complicates the situation because, besides the parameters which define the particles, the interaction between the particles becomes important in undiluted systems and simple linear extrapolation is no more possible. We have used diluted systems and have extracted our parameters from extrapolation to zero concentration or the limiting slope at zero concentration. The use of a diluted solution also allows appropriate correction for heterogeneity of our samples, which was small because of the precautions taken during the preparation of our samples (van den Oetelaar et al., 1985).

Three parameters define the interaction between hard spheres in solution: the size of the spheres, the repulsive interaction defined by the net charge of the particles and the interaction strength defined by the Debye length, and the attractive potential. From the extrapolated molar mass and diffusion coefficient, we have been able to calculate in an independent way the hydrodynamic radius of the particles. This turned out to be not influenced by the ionic strength, therefore the hydrodynamic volume does not change on changing the ionic strength.

By measuring the static coefficient K_I at different ionic strengths, we determined the net charge of the α-crystallin particles in the different solvent conditions. A change of the charges as a function of ionic strength is consistent with the physicochemical properties of proteins (Edsall and Wyman, 1958). These measurements also clearly suggest the presence of an attractive component in the interaction potential $V(x)$.

This attractive component is also evident from our light scattering measurements at high protein concentration and high ionic strength. An attractive component in the interaction parameter has been suggested from x-ray scattering measurements (Tardieu et al., 1987), but no quantitative data have been given.

For a long time it was thought that on aging, formation of drastic changes in the primary structure of the α-crystallin peptides were needed to increase light scattering of the eye lens cytoplasm, which could lead to senile cataract (Harding and Dilley, 1976). A change in the size of the α-crystallin aggregates, so that particles are formed with a size larger than λ/2, does increase light scattering (Benedek, 1971). For cold cataract, the formation of such large heterogeneity in the refractive index have been demonstrated (Delaye et al., 1982). For older lenses, the proof of the existence of larger aggregates as a consequence of biochemical changes has been indirect (Jedziniak et al., 1978; Siezen et al., 1979; Bloemendal, 1981).

It has been shown that in some cortical cataracts the malfunctioning of membrane ion channels is the only prominent feature (Duncan et al., 1989). It has also been shown that the progressive relative increase of permeability to sodium as a result of activation of nonspecific cation channels accompanies aging of the human lens and the development of age-related reduction in transparency (Maraini, 1991). These results are consistent with and can be explained by the interaction potential $V(x)$ as shown in Figure 6. Minor changes in the local pH, ionic strength, or concentration of some specific ions (such as Ca^{2+}) can dramatically change the interparticle interaction. This can result in a transition from repulsive to attractive interaction so that the formation of large aggregates occurs in a concentration-dependent way.

The formation of larger aggregates in α-crystallin solutions, on increasing the concentration of the protein, has been concluded from light scattering (Andries and Clauwaert, 1985). Nuclear magnetic relaxation dispersion measurements have also suggested the formation of large aggregates at a critical concentration of 15% of α-crystallin, similar to γ_{II}-crystallin (Koenig et al., 1992). This is consistent with the fact that both lens proteins have an attractive component in their interaction potential (which is much stronger for γ_{II} and takes place at much lower concentration). This aggregation and concomitant immobilization do not take place in β_L-crystallin solutions (Koenig et al., 1993) because of repulsive interaction (Tardieu et al., 1992).

REFERENCES

Andries, C., H. Backhovens, J. Clauwaert, J. De Block, F. De Voeght, and C. Dhont. 1982. Light-scattering and viscosity studies of low-molecular weight α-crystallin isolated from adult and embryonic bovine lenses. *Exp. Eye Res.* 43:239–255.

Andries, C., and J. Clauwaert. 1985. Photon correlation spectroscopy and light scattering of eye lens proteins at high concentrations. *Biophys. J.* 47:591–605.

Andries, C., W. Guedens, J. Clauwaert, and H. Geerts. 1983. Photon and fluorescence correlation spectroscopy and light scattering of eye-lens proteins at moderate concentrations. *Biophys. J.* 43:345–354.

Augusteyn, R. C., E. V. Parkhill, and A. Stevens. 1992. The effects of isolation buffers on the properties of α-crystallin. *Exp. Eye Res.* 54: 219–228.

Bender, T. M. R., R. J. Lewis, and R. Pecora. 1986. Absolute Rayleigh ratios of four solvents at 488 nm. *Macromolecules.* 19:244–245.

Benedek, G. B. 1971. Theory of transparency of the eye. *Appl. Optics.* 10:459–473.

Bloemendal, H. 1981. Molecular and Cellular Biology of the Eye Lens. John Wiley and Sons, New York. 469 pp.

Coopman, S., D. De Block, T. Aerts, W. Peeters, L. Moens, and J. Clauwaert. 1984. Physicochemical studies on bovine eye lens proteins. II. Comparative physical study of the low-molecular-weight α-crystallins from calf lens cortical and nuclear fiber cells. *Exp. Eye Res.* 38: 463–476.

Corti, M., and V. Degiorgio. 1981. Quasi-elastic light scattering of intermicellar interactions in aqueous sodium dodecyl sulfate solutions. *J. Phys. Chem.* 85:711–717.

Delaye, M., J. I. Clark, and G. B. Benedek. 1982. Identification of the scattering elements responsible for lens opacification in cold cataracts. *Biophys. J.* 37:647–656.

Delaye, M., and A. Gromiec. 1983. Mutual diffusion of crystallin proteins at finite concentrations: a light-scattering study. *Biopolymers.* 22: 1203–1221.

Delaye, M., and A. Tardieu. 1983. Short-range order of crystallins accounts for lens transparency. *Nature (Lond.).* 302:414–417.

Dorshow, R., and D. F. Nicoli. 1981. The effect of hydrodynamics on the diffusity of charged macromolecules: application to BSA. *J. Chem. Phys.* 75:5853–5856.

Duncan, G., K. R. Hightower, S. A. Gandolfi, J. Tomlinson, and G. Maraini. 1989. Human lens membrane cation permeability increases with age. *Invest. Ophthalmol. Visual Sci.* 30:1855–1859.

Edsall, J. T., and J. Wyman. 1958. Biophysical Chemistry. Vol. 1. Thermodynamics, Electrostatics and the Biological Significance of the Properties of Matter. Academic Press, New York. 699 pp.

Hamaker, H. C. 1937. The London-van der Waals attraction between spherical particles. *Physica.* IV:1058–1072.

Hansen, J. P., and J. B. Hayter. 1982. A rescaled MSA structure factor for dilute charged colloidal dispersions. *Mol. Physics.* 46:651–656.

Harding, J. J., and K. J. Dilley. 1976. Structural proteins of the mammalian lens: a review with emphasis on changes in development, aging, and cataract. *Exp. Eye Res.* 22:1–73.

Hayter, J. B., and J. Penfold. 1981. An analytical structure factor for macroion solutions. *Mol. Physics.* 42:109–118.

Jedziniak, J. A., D. F. Nicoli, H. Baram, and G. B. Benedek. 1978. Quantitative verification of the existence of high molecular weight aggregates in the intact normal human lens by light-scattering spectroscopy. *Invest. Ophthalmol. Visual Sci.* 17:51–57.

Koenig, S. H., R. D. Brown III, A. K. Kenworthy, A. D. Magid, and R. Ugolini. 1993. Intermolecular protein interaction in solutions of bovine lens β_L-crystallin. *Biophys. J.* 64:1178–1186.

Koenig, S. H., R. D. Brown III, M. Spiller, B. Chakrabarti, and A. Pande. 1992. Intermolecular interactions and conformation change in solutions of calf lens α-crystallin. *Biophys. J.* 61:776–785.

Koppel, D. 1972. Analysis of macromolecular polydispersity in intensity correlation spectroscopy: the method of cumulants. *J. Chem. Phys.* 31: 978–986.

Licinio, P., and M. Delaye. 1988. Direct and hydrodynamic interactions between α-crystallin proteins in dilute colloidal dispersions: a light scattering study. *J. Colloid Interface Sci.* 123:105–116.

Maraini, G. 1991. Membrane changes in the human lens during aging and cataract formation. *In* Eye Lens Membranes and Aging. Vol. 15. G. F. J. M. Vrensen and J. Clauwaert, editors. Eurage, Leiden. 45–57.

Ohshima, H., T. W. Healy, and L. R. White. 1982. Accurate analytical expression for the surface charge density/surface potential relationship and double-layer potential distribution for a spherical colloidal particle. *J. Colloid Interface Sci.* 90:17–26.

Ostrowsky, N., D. Sornette, P. Parker, and E. R. Pike. 1981. Exponential sampling method for light scattering polydispersity analysis. *Optica Acta.* 28:1059–1070.

Schurtenberger, P., and R. C. Augusteyn. 1991. Structural properties of polydisperse biopolymer solutions: a light scattering study of bovine α-crystallin. *Biopolymers.* 31:1229–1240.

Siezen, R. J., J. G. Bindels, and H. J. Hoenders. 1979. The interrelationship between monomeric, oligomeric and polymeric α-crystallin in the calf lens nucleus. *Exp. Eye Res.* 28:551–567.

Spector, A., and E. Katz. 1965. The deaggregation of bovine lens α-crystallin. *J. Biol. Chem.* 240:1979–1985.

Tabor, B. E. 1972. Preparation and clarification of solutions in light scattering. *In* Light Scattering from Polymer Solutions. M. B. Huglin, editor. Academic Press, London. 1–25.

Tanford, C. 1961. Physical Chemistry of Macromolecules. John Wiley and Sons, Inc., New York. 710 pp.

Tardieu, A., D. Laporte, and M. Delaye. 1987. Colloidal dispersions of α-crystallin proteins. I. Small angle x-ray analysis of the dispersion structure. *J. Physique.* 48:1207–1215.

Tardieu, A., D. Laporte, P. Licinio, B. Krop, and M. Delaye. 1986. Calf lens α-crystallin quaternary structure. A three-layer tetrahedral model. *J. Mol. Biol.* 192:711–724.

Tardieu, A., F. Vérétout, B. Krop, and C. Slingsby. 1992. Protein interactions in the calf eye lens: interactions between β-crystallins are repulsive whereas in γ-crystallins they are attractive. *Eur. Biophys. J.* 21: 1–12.

van den Oetelaar, P., J. Clauwaert, M. Van Laethem, and H. J. Hoenders. 1985. The influence of isolation conditions on the molecular weight of bovine α-crystallin. *J. Biol. Chem.* 260:14030–14034.

Vérétout, F., M. Delaye, and A. Tardieu. 1989. Molecular basis of eye lens transparency. Osmotic pressure and x-ray analysis of α-crystallin solutions. *J. Mol. Biol.* 205:713–728.

Vérétout, F., and A. Tardieu. 1989. The protein concentration gradient within the eye lens might originate from constant osmotic pressure coupled to differential interactive properties of the proteins. *Eur. Biophys. J.* 17:61–68.

Verwey E. J. W., and J. T. G. Overbeek. 1948. Theory of the Stability of Lyophobic Colloids. Elsevier Publishing Co., Amsterdam.205 pp.